Antarct. Meteorite Res., **16**, 105–127, 2003
© National Institute of Polar Research

Primitive clasts in the Dar al Gani 319 polymict ureilite: Precursors of the ureilites

Yukio Ikeda[1], Noriko T. Kita[2], Yuichi Morishita[2] and Michael K. Weisberg[3]

[1] *Faculty of Science, Ibaraki University, Mito 310–8512*
[2] *Geological Survey of Japan, AIST, Tsukuba Central 7, Tsukuba 305–8567*
[3] *Department of Physical Science, Kingsborough College (CUNY), 2001 Oriental Boulevard, Brooklyn, NY,11235, and Department of Earth and Planetry Sciences, American Museum of Natural History, New York, NY 10024, U.S.A.*

Abstract: Primitive clasts in the polymict ureilite Dar al Gani (DaG) 319 include dark clasts, sulfide- or metal-rich clasts, and unusual chondritic fragments. The dark clasts consist mainly of phyllosilicates, sulfides and magnetite with or without fayalitic olivine. The sulfide-rich clasts consist of a silicate-rich matrix and heterogeneously distributed sulfide. The metal-rich clasts consist of a silicate-rich matrix with variable amounts of metal. The unusual chondritic fragments are chondrule and equilibrated chondrite fragments.

Oxygen isotopic compositions of the silicate-rich matrices in the sulfide-rich or metal-rich clasts plot on the carbonaceous chondrite anhydrous mineral (CCAM) mixing line between Allende matrix and a dark clast in the Nilpena polymict ureilite. Their oxygen isotopic compositions are similar to those of the monomict ureilites. Considering its chondritic composition and oxygen isotopic composition, the silicate-rich matrix of the sulfide-rich clasts is the best candidate for the ureilite precursors. However, the matrix has an Mg/(Mg+Fe) ratio (mg ratio) of 0.56 and is too ferroan to produce the monomict ureilites with mg ratios of 0.74–0.95. Therefore, it may have experienced various degrees of reduction to produce precursors with the mg ratios, needed to form the monomict ureilites as residues during fractional melting.

Oxygen isotopic compositions of the unusual chondritic fragments plot near the ordinary chondrites on a 3-isotope diagram, suggesting that they have no direct genetic relationship to the monomict ureilites. They were projectiles that collided with the ureilite parent body (UPB).

key words: ureilites, DaG 319 polymict ureilite, primitive clasts, oxygen isotopes of clasts, ureilite precursors

1. Introduction

Ureilites are the second largest group of achondrites, next to the HED meteorites. They are classified into two major types, monomict and polymict. The monomict ureilites are more common and have simple mineral assemblages of olivine, pigeonite, and dark interstitial material containing carbonaceous materials, metal, sulfide and minor silicates, although some monomict ureilites have augite or orthopyroxene instead of pigeonite (Goodrich, 1992). The polymict ureilites are relatively rare, with five or more currently known (Cole *et al.*, 2002), and are more complex meteorites than

monomict ureilites. They are clastic matrix breccias, as defined by Stöffler *et al.* (1979), containing a variety of lithic clasts, including ureilitic clasts, igneous clasts, and primitive clasts (Jaques and Fitzgerald, 1982; Prinz *et al.*, 1983, 1986, 1987; Ikeda *et al.*, 2000).

Dar al Gani (DaG) 319 is a polymict ureilite found from the Libya desert and is the main focus of this study. Although ureilitic clasts are dominant in DaG 319, primitive (chondritic in composition) and igneous clasts are minor but important components. The primitive and igneous clasts never occur in monomict ureilites and provide critical clues to understanding ureilite petrogenesis.

One of the traditional problems concerning the origin of ureilites is whether they were produced by partial melting of chondritic precursors or by fractional crystallization of basaltic magmas (Goodrich, 1992). This problem has been discussed by many authors (Boynton *et al.*, 1976; Wasson *et al.*, 1976; Berkley *et al.*, 1980; Mittlefehldt, 1986; Goodrich *et al.*, 1987; Takeda, 1987; Rubin, 1988; Kurat, 1988; Warren and Kallemeyn, 1989; Scott *et al.*, 1992; Walker and Grove, 1993) and in our companion paper (Ikeda and Prinz, 2001), which dealt with igneous clasts in DaG 319. Recently, Singletary *et al.* (2002) presented new evidence from melting experiments supporting a fractional melting origin of monomict ureilites, and Goodrich *et al.* (2002) discussed a new model for polymict ureilites representing a regolith breccia developed on a reassembled parent body. Another major issue is deciphering the precursor material from which ureilites formed. Oxygen isotopic compositions of whole rock monomict ureilites do not form a mass fractionation line, and instead form a mixing line which is an extension of the CCAM mixing line of the Allende meteorite (CV3). This suggests that they are relatively unprocessed, primitive materials (Clayton and Mayeda, 1988). However we do not know what kind of chondritic materials they are related to. In this paper we examine primitive lithic clasts in the DaG 319 polymict ureilite, which may be relicts of the ureilite precursors.

2. Analytical method

Chemical compositions of constituent minerals and glass were analyzed by an electron-probe microanalyzer (EPMA), using a focused beam at an accelerating voltage of 15 kV. A beam current of 3 nA and a counting time of 10 s were used for glass, carbonates, phosphates, and phyllosilicates to suppress evaporation of volatile components such as alkalis, and 10 nA and 20 s were used for ferromagnesian silicates, oxides, metal and sulfides. The detection limits for the former condition are shown in Ikeda *et al.* (2000), and those for the latter case are about 0.05 wt% for TiO_2, Cr_2O_3, FeO, MnO, CaO, Na_2O, and K_2O, and about 0.02 wt% for SiO_2, Al_2O_3 and MgO. Analyses except metal and sulfides were corrected using the Bence and Albee (1968) method, and metal and sulfides using the standard ZAF method.

A defocused beam with a diameter of 50 μm was employed for bulk analyses of primitive clasts. The primitive clasts consist of silicate-rich materials with variable amounts of metal and sulfides, and the silicate-rich portions were analyzed. The silicate-rich materials in some primitive clasts (sulfide-rich or metal-rich clasts, and equilibrated chondrite fragments) are coarse-grained with grain sizes larger than several

microns, and they are larger in size than the depth of X-ray emission area of a few microns during defocused beam analyses of EPMA. Therefore, these analyses were corrected by the method of Ikeda (1980). The other primitive clasts (dark clasts) consist mainly of fine-grained minerals with grain sizes smaller than a few microns. Defocused EPMA data for these dark clasts were corrected using the Bence and Albee method, and the special correction for the defocused beam analyses was not applied. A beam current of 10 nA and a counting time of 20 s were used for the defocused beam analyses. The detection limits are dependent upon conditions of grain boundaries and fractures in clasts and amounts of tiny opaque minerals (sulfides or metal) that can not be avoided from the defocused beam, and may be about 10 times larger than those for the focused beam analyses above stated. More than 10 points were analyses for a clast, and they are averaged.

Oxygen isotopic compositions of clasts were measured with a high sensitivity and high resolution SIMS (secondary ion mass spectrometer, IMS-1270) at the Geological Survey of Japan. Cs^+ primary ion ($+20$ kV) was shaped as a 10 μm spot on the sample surface with ~0.7 nA ion intensity. The secondary ion of O^- was sputtered from a sample surface (-10 kV). An incident electron gun (-10 kV) was used for charge compensation. The mass resolution power was set to 4500 in order to separate OH^- molecular interference fully from ^{17}O. All three oxygen isotopes were measured with three Faraday cup detectors simultaneously by combining two multi-collectors and the mono collector. The secondary ^{16}O ion intensity was set to ~6×10^8 cps (or 1×10^{-10} A) and the stability of baseline of Faraday detectors were as low as 10^3 cps. The internal errors of single analysis were 0.3‰ and 1‰ for $\delta^{18}O$ and $\delta^{17}O$, respectively. The instrumental fractionation factors of the SIMS were estimated by measuring terrestrial olivine and pyroxene standards with known $\delta^{18}O$. Repeated analysis of terrestrial standards gave the reproducibility of 0.3–0.5‰ for $\delta^{18}O$ within a day.

3. Petrology of primitive clasts in DaG 319

DaG 319 consists mainly of lithic clasts and isolated mineral fragments. Six thin sections of DaG 319 were prepared, and more than 200 lithic clasts were inspected in details. Most clast types are ureilitic, and they are large up to 1 cm across. Primitive clasts are minor in DaG 319.

Primitive clasts are classified into three types: dark clasts, sulfide- or metal-rich clasts, and unusual chondritic fragments, and each type is further subdivided into two subtypes. They are listed in Table 1, where each type is designated by letters D (Dark clasts), E (sulfide- or metal-rich clasts), or F (unusual chondritic fragments), and the subtypes are designated with numbers, for example D1 and D2. There are more than 30 dark clasts and 10 unusual chondritic clasts in the six thin sections inspected. But sulfide- and metal-rich clasts are very rare, and each is a few in number. Brief descriptions of primitive clasts in DaG 319 are presented by Ikeda *et al.* (2000), and detailed petrography and mineralogy are given below.

3.1. Dark clasts (D)

The dark clasts are aggregates consisting mainly of phyllosilicates, magnetite, and

sulfide (Fig. 1A). They are angular in shape and range from a few hundred micrometers to a few millimeters in size. Dark clasts in DaG 319 are subdivided into two types, Fa-free and Fa-bearing (Table 1). The Fa-free subtype is enriched in phyllosilicates and often contains phyllosilicate veins. The Fa-bearing subtype contains small fayalitic olivine grains in the matrix, and phyllosilicates occur in small amounts. No phyllosilicate veins occur in this subtype.

3.1.1. Fa-free subtype (D1 in Table 1)

The Fa-free subtype appears to be completely hydrated, consisting mainly of a phyllosilicate-rich matrix with variable amounts of opaque minerals (sulfides and magnetite), carbonate fragments, and phyllosilicate nodules (Fig. 1A). Some clasts of this subtype contain anhydrous silicates such as olivine, pigeonite and rhyolitic glass (Ikeda *et al.*, 2000), which may be exotic minerals that were mechanically mixed into the dark clasts after they formed. The matrix is dominated by phyllosilicates and contains fine grains of euhedral to subhedral pyrrhotite, subrounded magnetite, and tiny ($<1\mu$m) phosphate. In some cases, the matrix shows pseudomorphic textures of previous anhydrous minerals which were replaced by phyllosilicates (Fig. 1B). Phyllosilicate veins occur in some Fa-free clasts (Ikeda *et al.*, 2000). Thus, the phyllosilicates of DaG 319 occur as matrix, nodules, and veins. Chemical compositions of the phyllosilicates are shown in Table 2 and Fig. 2. They seem to be a mixture of a large amount of serpentine and a small amount of smectite accompanied by Fe oxides or sufides. The Al_2O_3 contents of the phyllosilicates range from 0.5 to 6.0 wt%; low-Al phyllosilicates with $Al_2O_3 < 3.5$ wt% are more abundant than the high-Al phyllosilicates with $Al_2O_3 > 3.5$ wt%. High-Al phyllosilicate veins cut low-Al phyllosilicate veins, suggesting that high-Al ones formed later. Low-Al ones may be mostly serpentine, and high-Al ones may be smectite-rich. Magnetite in some clasts occurs as subrounded or

Table 1. Classification of lithic clasts in polymict ureilites.

(Ⅰ)	Ureilitic Clasts
	(A) Coarse-grained Mafic Clasts
	(B) Fine-grained Mafic Clasts
(Ⅱ)	Igneous Clasts
	(C) Felsic Clasts
(Ⅲ)	Primitive Clasts
	(D) Dark Clasts
	(D1) Fa-free Type
	(D2) Fa-bearing Type
	(E) Sulfide or Metal-rich Clasts
	(E1) Sulfide-rich Clasts
	(E2) Metal-rich Clasts
	(F) Unusual Chondritic Fragments
	(F1) Chondrule Fragments
	(F2) Equilibrated Chondrite Fragments
(Ⅳ)	Isolated Mineral Clasts
	(G) Mineral Clasts

Ureilitic (Ⅰ) and igneous (Ⅱ) clasts are described in Ikeda *et al.* (2000) and Ikeda and Prinz (2001).

framboidal grains, and is poor in MnO and MgO (<0.5 wt%). Ilmenite also occurs rarely in the Fa-free subtype, and it is rich in MnO (4–5 wt%) and poor in MgO (<0.5 wt%) in comparison with those in the igneous felsic clasts (1.0–1.5 wt% MnO and 3.0–4.5 wt% MgO). Carbonates in the Fa-free subtype consist of dolomite and magnesite, and are rich in MnO, being similar to those in the CI chondrites (Ikeda *et al.*, 2000). Calcite veins, several micrometers wide, cut through many lithic clasts and the matrix, indicating that they formed after the formation of the DaG 319 polymict ureilite. It is likely that these calcite veins are products of terrestrial alteration.

The Fa-free subtype is similar to dark inclusions that occur in some carbonaceous chondrites. However, the dark clasts in DaG 319 do not contain chondrules, unlike some chondrule-bearing dark inclusions in carbonaceous chondrites. Brearley and Prinz (1992) concluded that phyllosilicate-rich dark clasts in Nilpena are texturally similar to CI chondrites, but differ to some extent from CI chondrites in mineralogy. They suggested that the CI-like dark clasts represent a component of a late-accreting veneer on the UPB. The Fa-free dark clasts in DaG 319 may be a kind of CI chondrite, supporting the conclusion of Brearley and Prinz (1992). However, the dark clasts contain abundant phyllosilicate veins and nodules, which are not common in typical CI chondrites such as the Orgueil meteorite.

3.1.2. Fa-bearing subtype (D2 in Table 1)

Fa-bearing subtype of dark clasts consists mainly of a silicate-rich matrix with opaque minerals (sulfides and magnetite) and exotic fragments (Fig. 1C). The matrix is mainly composed of phyllosilicate, with minor amounts of fayalitic olivine ($Fa_{>70}$) and tiny (μm-size) opaque minerals (magnetite and sulfide). The chemical compositions of the matrix phyllosilicate and fayalite are shown in Table 2 and Figs. 2 and 3. In comparison with the matrix phyllosilicates in the Fa-free subtype, ferroan phyllosilicates, smaller than 0.7 mg ratios, are dominant in Fa-bearing subtype, and minor magnesian phyllosilicates with mg ratios >0.7 are more enriched in SiO_2 and Al_2O_3 (Fig. 2). These data suggests that the phyllosilicates in the Fa-bearing dark clasts contain a larger amount of smectite component than those in the Fa-free type. The matrix of the Fa-bearing type is more porous than that of the Fa-free type, and appears to be ill crystalline. Some of the fayalitic olivine shows reverse zoning from ferroan core (Fa_{90-100}) to less-ferroan rims (Fa_{75-90}).

The Fa-bearing subtype contains exotic rock and mineral fragments. They may be either igneous rock fragments or chondrule fragments (Fig. 1C, D), and their derivative mineral fragments, as well as forsterite fragments of $Fo_{>97}$. Generally speaking, chondrules are defined to be rounded-shaped silicate melt droplets. However, the exotic rock fragments in the Fa-bearing subtype are angular in shape. Therefore, it is not clear whether they are fragments of picritic basalts or peridotites or fragments of chondrules.

Some exotic rock fragments contain olivine phenocrysts, which show normal zonation from magnesian cores (Fo_{85-90}) to ferroan rims (Fo_{75-80}) and rarely have a core of relict forsteritic olivine (Fo_{97-100}). The groundmass contains phyllosilicate and minor amounts of fayalite, as well as fine-grained augite and olivine with compositions of Fo_{50-60} (Fig. 1D). The fragment was slightly hydrated, and the groundmass glass was altered to phyllosilicates associated with minor amounts of fayalitic olivine and

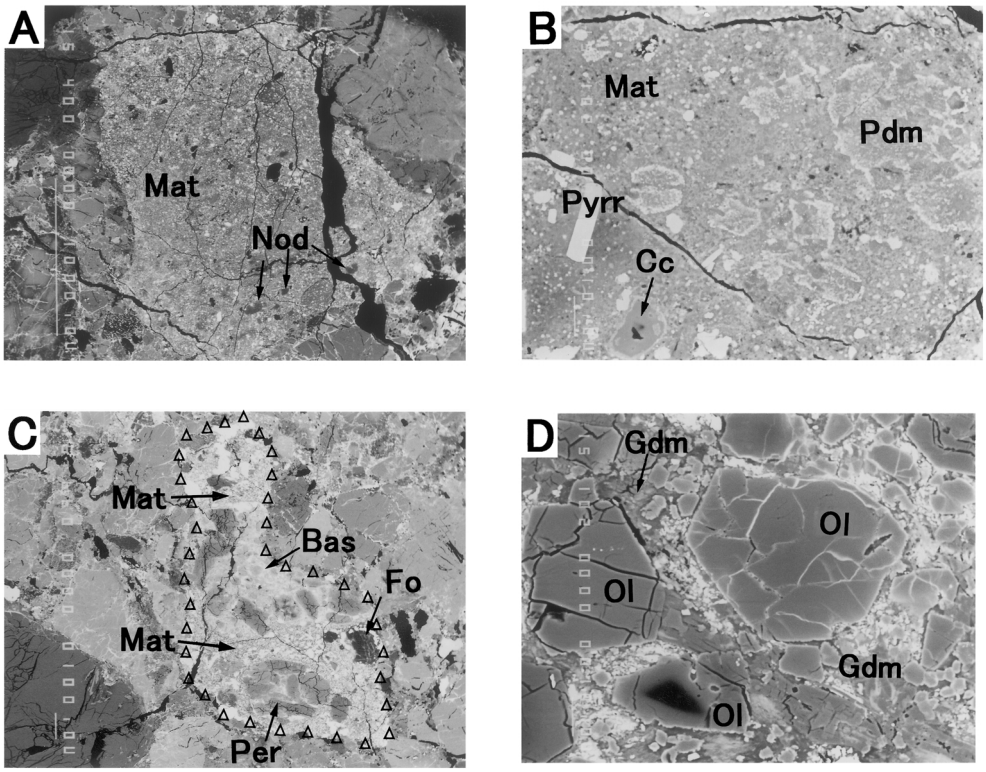

Fig. 1. Back scattered electron (BSE) images of primitive lithic clasts in DaG 319.

(A) Fa-free dark clast consisting mainly of phyllosilicate-rich matrix (Mat), phyllosilicate nodules (Nod) and small grains of sulfide or magnetite (white dots). Field of view = 3 mm.

(B) Enlarged BSE image of a Fa-free dark clast, showing phyllosilicate-rich matrix (Mat) and pseudomorphs (Pdm) replaced by fine-grained aggregates of phyllosilicates and Fe-phases. Pyrrhotite (Pyrr) often shows elongated euhedral forms and calcite (Cc) is a terrestrial weathering product. Field of view = 120 μm.

(C) A Fa-bearing dark clast is surrounded by a chain of open triangles. It contains exotic rock fragments (picritic basalt or chondrule (Bas), peridotite or chondrite (Per), and forsterite (Fo)) set in phyllosilicate-rich matrix (Mat). Fayalitic olivine occurs in the matrix. Field of view = 1.9 mm.

(D) Enlarged BSE image of an exotic rock fragment (picritic basalt or chondrule) in (C), consisting of phenocrystic olivine (Ol) and groundmass (Gdm). The phenocrystic olivine often shows normal zoning from magnesian cores to ferroan rims, and a lower left olivine grain shows remarkable zonation. The groundmass is hydrated, consisting mainly of phyllosilicates and magnetite with minor fayalite, as well as primary anhydrous groundmass minerals such as olivine and pyroxenes. Field of view = 120 μm.

magnetite, showing the same mineral assemblage as matrix in the host Fa-bearing clasts. The hydration of the groundmass in the exotic rock fragments may have taken place at the same time with that of the Fa-bearing clasts, after its incorporation with the host clasts. An exotic rock fragment consists mainly of olivine of Fo_{82-85} and orthopyroxene with minor amounts of augite and is peridotitic. The chemical compositions of olivine

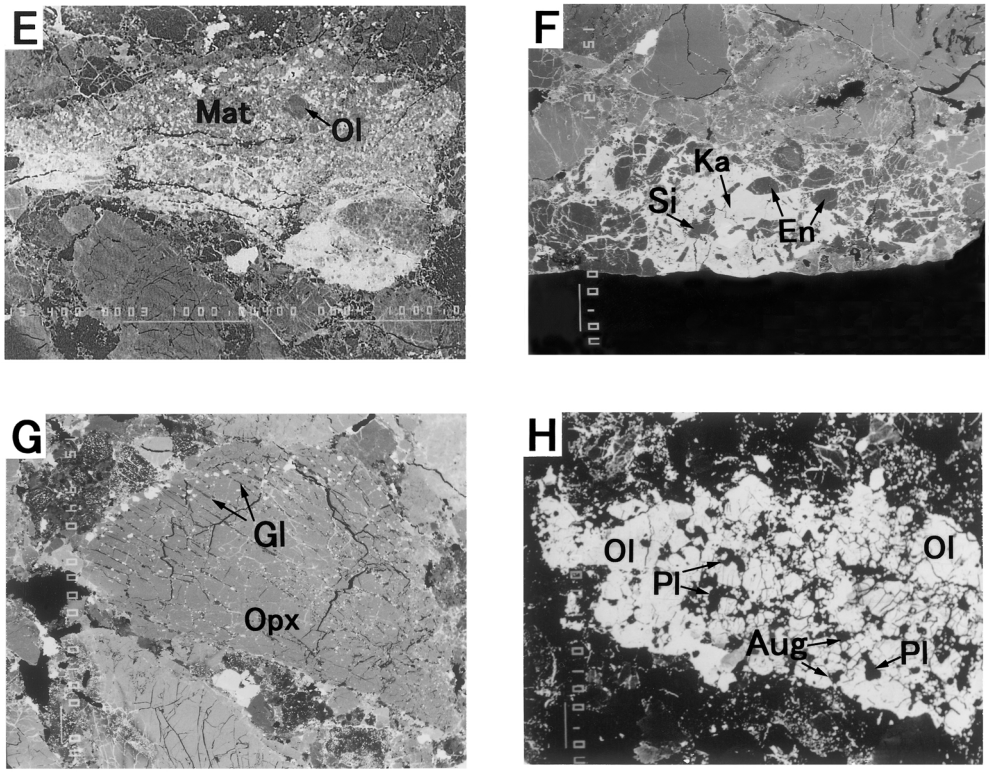

Fig. 1 (continued).

(E) Sulfide-rich clast consisting mainly of silicate-rich matrix (Mat), large olivine grains (Ol), and sulfide (white phase). Field of view=3.8 mm.

(F) Metal-rich clast consisting mainly of enstatite (En), kamacite (Ka), and a silica mineral (Si). Field of view=1 mm.

(G) A chondrule fragment consisting mainly of radial orthopyroxene (Opx), devitrified glass (Gl), sulfide (white spots in the chondrule), and minor olivine occurring at the edge. Tiny metal are rarely included in orthopyroxene. Field of view=1.36 mm.

(H) Equilibrated chondrite fragment consisting mainly of olivine (Ol), augite (Aug), plagioclase (Pl), chromite and sulfide. Field of view=1 mm.

in the exotic rock fragment are shown in Table 2 and Fig. 3. Chemical compositions of some forsterite fragments in the Fa-bearing clast are also shown in Fig. 3. The CaO content of the forsterite is high, in comparison with olivine ($Fo_{<90}$) in the exotic rock fragments. This Fa-bearing subtype seems to represent an early stage of hydration of chondritic materials. Nearly pure fayalitic olivines were described in the oxidized CV chondrites (Kaba, Bali,Mokoia) which experienced hydration (Hua and Busec, 1995; Weisberg *et al.*, 1998; Krot *et al.*, 1998,2000; Choi *et al.*, 2000). The fayalites in dark clasts in DaG 319 may have been produced by a similar formational mechanism to those in the CV chondrites. They might be a new type of chondrule-free carbonaceous chondrites related to CV chondrites.

Table 2. Average chemical compositions of minerals in primitive lithic clasts in DaG 319.

	Fa-free Dark Clast		Fa-bearing Dark Clast				Sulfide-rich Clast	
	vein-PS lowAl PS	vein-PS highAl PS	Mat-PS highAl PS	Fayalite Fa98	Exotic frag (Fo85-90)	Fo-frag Fo100	ferroan Ol (Fo48-51)	Mg-Ol (Fo90-85)
SiO_2	38.34	36.87	40.31	29.73	41.08	43.01	34.35	40.84
TiO_2	bd	bd	0.06	bd	bd	bd	bd	bd
Al_2O_3	2.28	4.81	5.03	0.04	bd	bd	0.02	bd
Cr_2O_3	1.25	0.52	0.43	bd	0.33	0.17	0.07	0.21
FeO	14.15	18.60	16.45	67.77	11.21	0.47	40.85	12.18
MnO	0.13	0.20	0.14	0.55	0.28	0.05	0.37	0.17
MgO	28.90	23.56	22.34	0.87	46.80	55.92	22.84	46.53
CaO	0.71	0.92	0.77	0.02	0.10	0.30	0.19	0.05
Na_2O	0.62	0.92	0.81	bd	bd	bd	bd	0.05
K_2O	bd	0.51	0.49	bd	bd	bd	bd	bd
Total	86.38	86.91	86.83	98.98	99.80	99.92	98.69	100.03

	Metal-rich Clast		Chondrule Fragment			Eq. Chondrite Frag	
	Relic Ol Fo82	En	homog. Ol Fo72	zoned Ol (Fo97-95)	zoned Ol (Fo80-73)	homog. Ol Fo68	homog. Ol Fo59
SiO_2	40.14	59.98	37.51	42.81	39.57	37.24	37.12
TiO_2	bd	bd	bd	bd	bd	bd	bd
Al_2O_3	bd	0.07	bd	0.03	bd	bd	bd
Cr_2O_3	0.20	0.05	bd	0.50	0.25	bd	bd
FeO	16.65	0.76	25.05	3.47	20.27	27.89	35.01
MnO	0.48	0.01	0.43	0.22	0.41	0.42	0.38
MgO	43.01	39.61	36.50	52.86	39.41	33.76	28.14
CaO	0.14	0.08	0.05	0.18	0.11	0.07	bd
Na_2O	bd	bd	bd	bd	bd	bd	bd
K_2O	bd	bd	bd	bd	bd	bd	bd
Total	100.62	100.56	99.54	100.07	100.02	99.38	100.65

Abbreviation: fayalite (Fa), phyllosilicates (PS), low-Al (lowAl), high-Al (highAl), matrix (Mat), fragments (frag), forsterite (Fo), magnesian olivine (Mg-Ol), enstatite (En), equilibrated (Eq.), homogeneous (homog), and below detection (bd).

3.2. Sulfide or metal-rich clasts (E)

Sulfide-rich and metal-rich clasts are very rare in DaG 319, but they stand out in thin section because of their abundant sulfide or metal. Although the sulfide or metal constitutes more than 20 vol%, it is heterogeneously distributed in the clasts, and their modal abundances are variable among clasts.

3.2.1. Sulfide-rich clasts (E1 in Table 1)

Sulfide-rich clasts consist mainly of a silicate-rich matrix and sulfides (Fig. 1E). The silicate-rich matrix is dominated by olivine grains and is porous; it is similar in texture to the Allende (CV3) chondrite matrix, but the former is coarser than the latter. Olivine shows normal chemical zoning from magnesian core (Fo_{80-90}) to ferroan rim (Fo_{50-70}). The CaO and Cr_2O_3 contents of the olivine in the sulfide-rich clasts (Table 2, Fig. 4) are different from those in ureilitic lithologies (CaO of 0.2–0.4 wt% and Cr_2O_3 of 0.4–0.7 wt%) with mg ratios of 0.75–0.90 (Ikeda *et al.*, 2000). Troilite

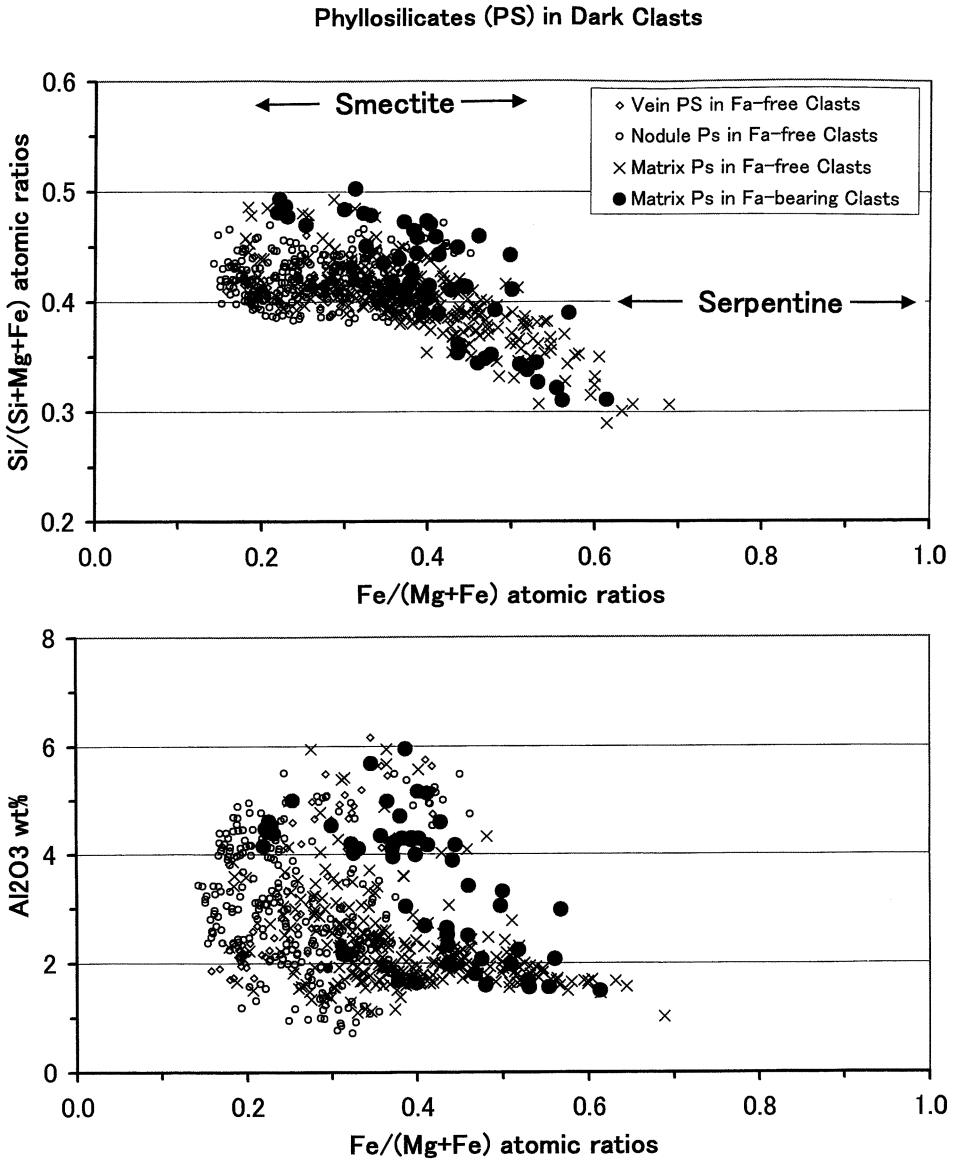

Fig. 2. Chemical compositions of phyllosilicates occurring as veins, nodules, and matrix in the Fa-free dark clasts, as well as matrix phyllosilicates in the Fa-bearing dark clasts. Compositional ranges of smectite and serpentine are shown for reference.

is the major phase in this type of clasts and it is disseminated into the silicate-rich portions (Fig. 1E). Metal is rare and it is high-Ni metal with Ni = 10–23 wt%, which may be metastable.

3.2.2. Metal-rich clasts (E2 in Table 1)

Metal-rich clasts consist mainly of enstatite and metal with variable amounts of a

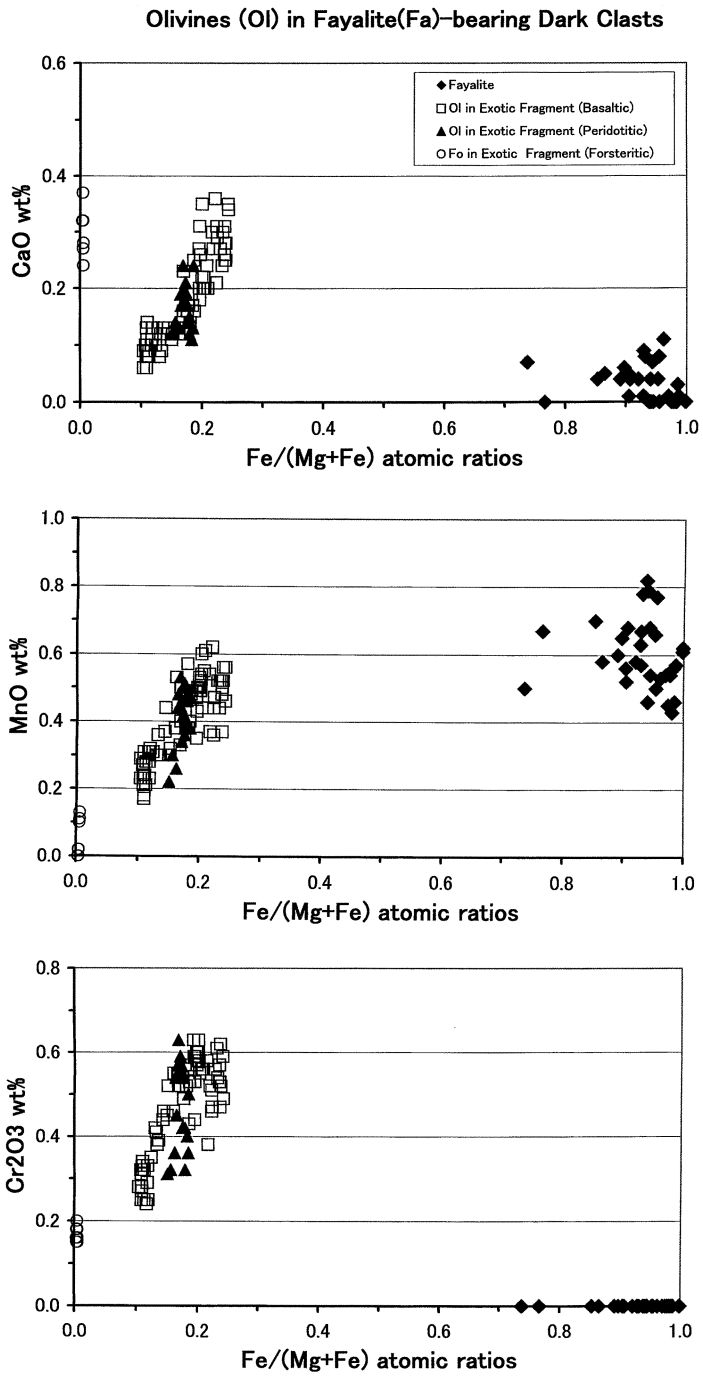

Fig. 3. Fayalites in a Fa-bearing dark clast are shown together with olivines (Ol, mg = 0.75–0.90) in exotic rock fragments (basaltic and peridotitic), as well as forsterite (Fo, mg > 0.97) fragments in the dark clast.

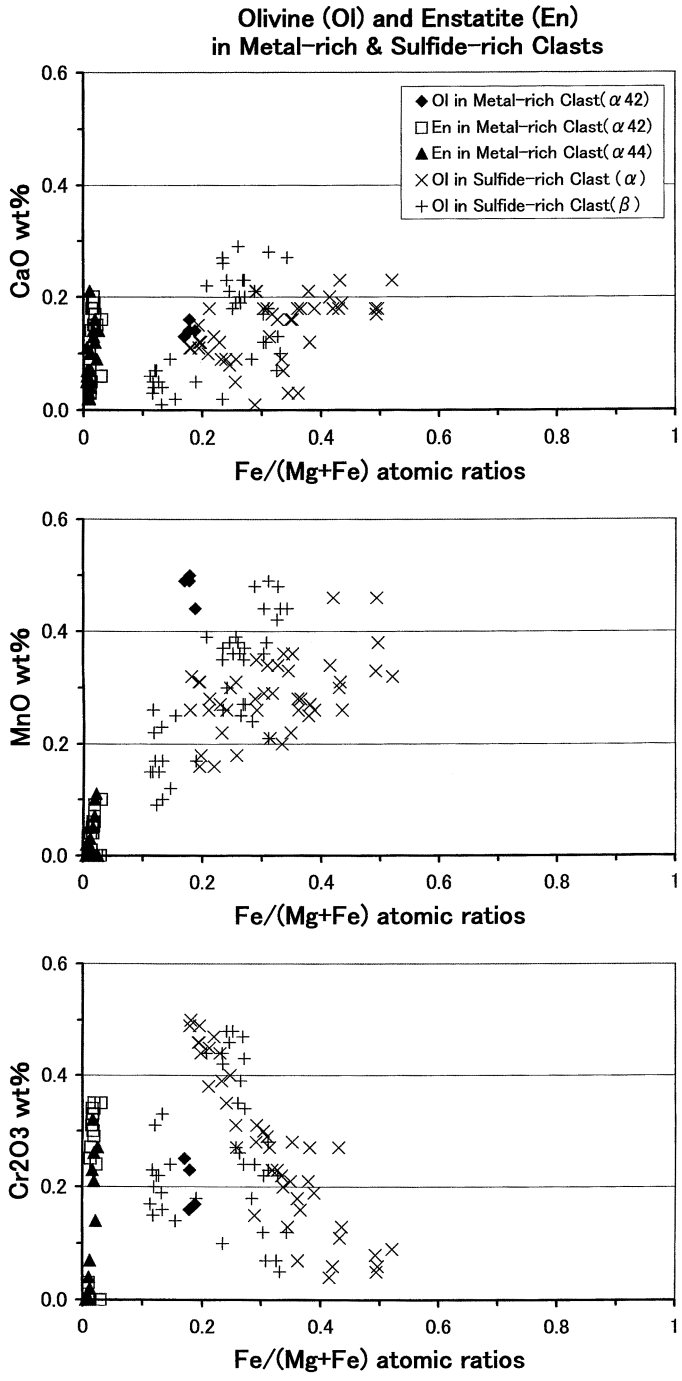

Fig. 4. Olivines (Ol) in two sulfide-rich clasts (α and β) show chemical zoning from magnesian core to ferroan rims, and enstatites (En) in two metal-rich clasts (α42 and α44) are plotted at the left end of the horizontal axes with reference of relic olivines in a metal-rich clast (α42).

silica mineral, plagioclase, sulfide, and rarely olivine (Fig. 1F). They are fine-grained, grain sizes ranging from several to several tens of micrometers. Some large enstatite grains (several tens of micrometers) in the fine-grained type contain aggregates of submicrometer-size minerals in their cores. Broad beam analyses by an EPMA show that the aggregates have a chemical composition of hypersthene, suggesting that they may be mixtures of tiny enstatite, metal and silica. In one clast, a few small grains of Fe-bearing olivine (Fo_{79-83}) occur completely enclosed by sulfide. Since the clast is enriched in a silica mineral, these olivine grains may be relic crystals. Compositions of the enstatite and relic olivine in the metal-rich clasts are shown in Table 2 and Fig. 4. The major metal phase is kamacite with Si = 2–4 wt%, but most of it has been altered to limonitic weathering products. The major sulfide phase is troilite, with Cr = 0.4 to 7.0 wt%; pentlandite, with Ni up to 20 wt% and negligible Cr, is a minor phase.

3.3. Unusual chondritic fragments (F)

Unusual chondritic fragments in DaG 319 include chondrule and equilibrated chondrite fragments. They are called unusual, because they have oxygen isotopic similarities to the ordinary chondrites as discussed later, but the equilibrated chondritic fragments have highly ferroan silicates similar to R chondrites, as shown below. The chondrule fragments contain clear or devitrified glass, whereas equilibrated chondrite fragments contain plagioclase. The chondrule fragments are similar in texture and mineralogy to chondrules in ordinary chondrites.

3.3.1. Chondrule fragments (F1 in Table 1)

The chondrule fragments in DaG 319 (Fig. 1G) include barred olivine, porphyritic olivine, porphyritic olivine-pyroxene, and radial pyroxene chondrules. The major minerals are olivine and/or low-Ca pyroxene with minor amounts of augite. Olivine in some chondrules shows normal zoning from magnesian core to ferroan rim, but those in other chondrules are homogeneous in compositions (Table 2 and Fig. 5). The CaO, MnO and Cr_2O_3 contents of olivines in the chondrule fragments are similar to those of olivine in chondrules from type 3 ordinary chondrites (Brearley and Jones, 1998). The groundmass is devitrified or glassy and albitic in composition, and it is similar to chondrule mesostasis in ordinary chondrites (Ikeda, 1980). Troilite is a minor component in the chondrule fragments in DaG 319, and metal is rare, occurring as tiny grains included in silicates. The tiny metal grains contain 10–20 wt% Ni. The chondrule fragments in DaG 319 are similar in texture and mineral composition to chondrules in ordinary chondrites.

3.3.2. Equilibrated chondrite fragments (F2 in Table 1)

The equilibrated chondrite fragments consist mainly of olivine, orthopyroxene, augite, and plagioclase with minor amounts of sulfide (Fig. 1H). Olivine is the dominant mineral in the chondrite fragments, and pyroxene is minor. Both are homogeneous in composition, and the olivines are Fo_{59-68} although they differ among fragments (Table 2 and Fig. 5). The CaO, MnO, and Cr_2O_3 contents of olivine are similar to those in equilibrated ordinary chondrites, as shown in Fig. 5, but their mg ratios are smaller than the latter (0.68–0.84). The plagioclase occurs interstitially to olivine and pyroxene grains, and is similar in texture to plagioclase in equilibrated ordinary chondrites (Van Schmus and Ribbe, 1968). It is An_{6-11} Or_{5-8}, and the grain

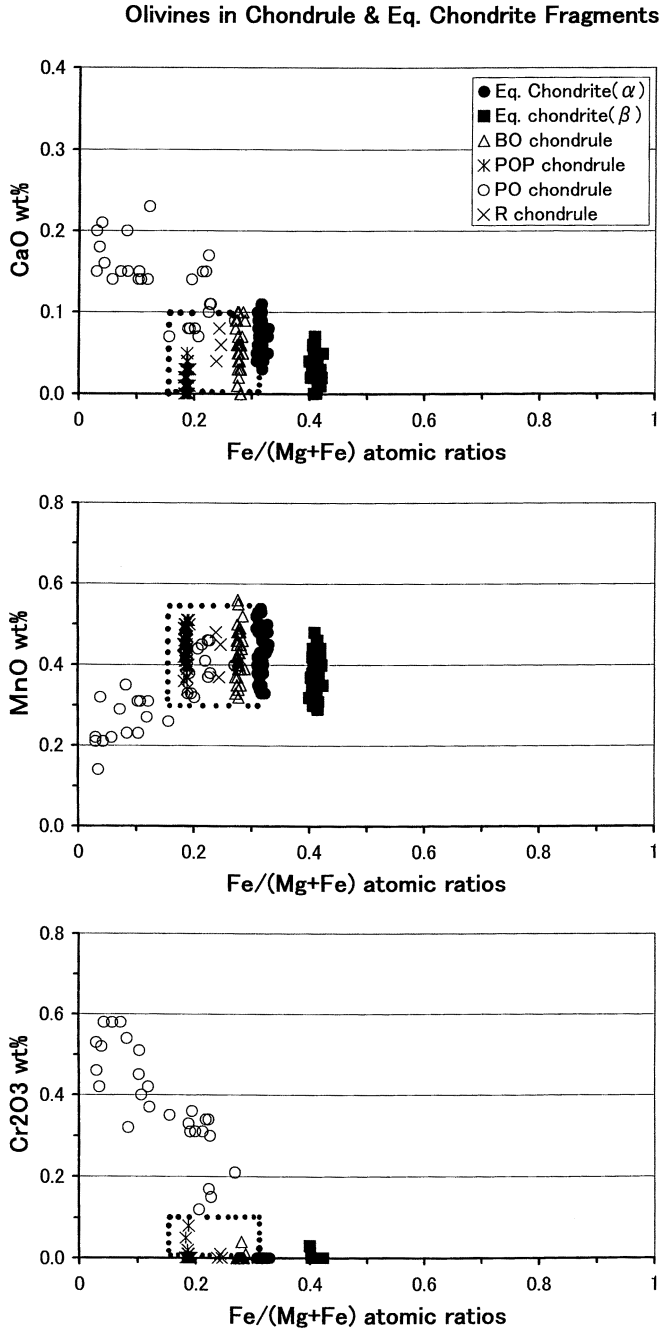

Fig. 5. Composition of olivines (Ol) in four chondrule fragments (barred Ol, porphyritic Ol-pyroxene, porphyritic Ol, and radial pyroxene chondrules) and in two equilibrated chondrite fragments (α and β). Compositional ranges of olivines in some equilibrated ordinary chondrites (Y-74492 (H6), Y-74014 (H6), ALH-77272 (L6), Y-74118 (L6), Y-74646 (LL6)) are shown for reference by dotted boxes.

size is several to a few tens of microns. The grain size is smaller than that in type 6 of ordinary chondrites, suggesting that it may correspond to a lower petrological type (4 or 5). Chromite occurs in an equilibrated chondrite fragment, and both the Al_2O_3 and TiO_2 are about 5–6 wt%. The Al_2O_3 content is similar to that in ordinary chondrite chromite, but the TiO_2 content is slightly higher than that in ordinary chondrite chromite with TiO_2 of 2–4 wt%. Sulfide is troilite and pentlandite, and is very scarce in the equilibrated chondrite fragments, in comparison with ordinary chondrites. The pentlandite has high Ni contents of 32–34 wt%. Metal and magnetite are absent in the chondrite fragments.

Olivine in the equilibrated chondrite fragments in DaG 319 has mg ratios similar to that in R and CK group chondrites. However, plagioclase in CK is more calcic than that in the equilibrated chondrite fragments in DaG 319, and magnetite is absent in the fragments, suggesting the equilibrated chondrite fragments differ from the CK chondrite group. The equilibrated chondrite fragments in DaG 319 are similar in petrology to R chondrites. Olivine in the R group is ferroan with Fo_{58-63}, their plagioclase is sodic with An_{7-12}, the amount of sulfides is very little, their chromian spinel contains high TiO_2 (5–6 wt%), and metals and magnetite were not detected in R group (Rubin and Kallemeyn, 1989; Weisberg *et al.*, 1991; Bischoff *et al.*, 1994). Then, the equilibrated chondrite fragments have textures and mineral compositions similar to R chondrites.

4. Bulk compositions of the primitive clasts

Major elemental chemical compositions of the silicate-rich portions in some primitive clasts in DaG 319 were obtained by a defocused beam EPMA technique. One to ten clasts were measured for each subtype, and they were averaged to obtain a representative composition for the subtype.

4.1. Dark clasts

The bulk compositions of ten Fa-free clasts were obtained, and the average value is shown in Table 3 and Fig. 6. The S is contained in about 1 wt%, because tiny grains of sulfide occur in the matrix. The Si-normalized composition is similar to that of CI chondrite (Fig. 6), but the Na content of the Fa-free type is depleted in comparison with CI chondrite.

Average composition of matrices in two Fa-bearing clasts is shown in Table 3 and Fig. 6. It is very similar in composition to the matrix of the Fa-free subtype, but the S content is higher, probably due to abundant tiny sulfide grains in the matrix of the Fa-free type. The Na and K contents of the matrix in the Fa-bearing type are richer than those in the Fa-free type (Table 3).

4.2. Sulfide-rich and metal-rich clasts

Chemical compositions of the silicate-rich matrices in two sulfide-rich clasts were measured, and the average is shown in Table 3 and Fig. 6. It is very similar in major element composition to CI chondrite. Chemical compositions of silicate-rich matrices in a metal-rich clast were also obtained. Their average composition is poor in Ca, Mn, Fe, and Ni in comparison with the silicate-rich matrices of the other clast type. This

Table 3. Average chemical compositions of silicate-rich portions (obtained using broad-beam EPMA) in primitive clasts in DaG 319. The chemical composition of the Allende matrix obtained by McSween and Richardson (1977), using broad beam EPMA, is shown for comparison.

	Dark clasts		Sulf-rich clasts	Met-rich clasts	Eq. chondrite fragments		Allende
	Fa-free	Fa-bearing	Sil-rich matrix	Sil-rich matrix	(α43A)	(β22B)	matrix
SiO_2	30.1	32.0	35.1	49.2	40.8	37.7	28.0
TiO_2	0.1	0.0	0.1	0.0	0.0	0.0	0.09
Al_2O_3	1.9	2.7	2.5	1.0	1.3	2.1	2.30
Cr_2O_3	0.5	0.4	0.8	0.5	0.3	0.4	0.38
FeO	24.9*	26.8*	32.1*	13.2*	25.5	29.8	31.9
NiO	1.3**	1.5**	0.7**	0.5**	0.8**	0.7**	1.83
MnO	0.2	0.2	0.3	0.1	0.3	0.3	0.21
MgO	19.8	20.7	22.6	31.7	25.2	24.0	20.2
CaO	1.6	1.6	2.0	0.3	1.5	1.3	2.37
Na_2O	0.2	0.5	0.7	0.5	0.5	0.8	0.22
K_2O	0.1	0.2	0.1	0.0	0.1	0.1	0.01
P_2O_5	0.3	0.3	0.5	0.0	0.1	0.1	—
S	1.0	2.4	0.5	0.8	0.5	0.3	1.13
Total	82.0	89.3	98.0	97.8	96.9	97.6	88.64

Silicate-rich (Sil-rich) matrix of sulfide-rich and metal-rich clasts and equilibrated (Eq) chondrite fragments were corrected by method of Ikeda (1980), because they are coarse-grained multi-phase aggregates.

*Fe may be partly in magnetite, sulfide, or metal phases in addition to silicates, **Ni is mainly in sulfide or metal phases, and S in sulfide phases. Total wt% of dark clasts are low, because of the water-bearing phyllosiicates.

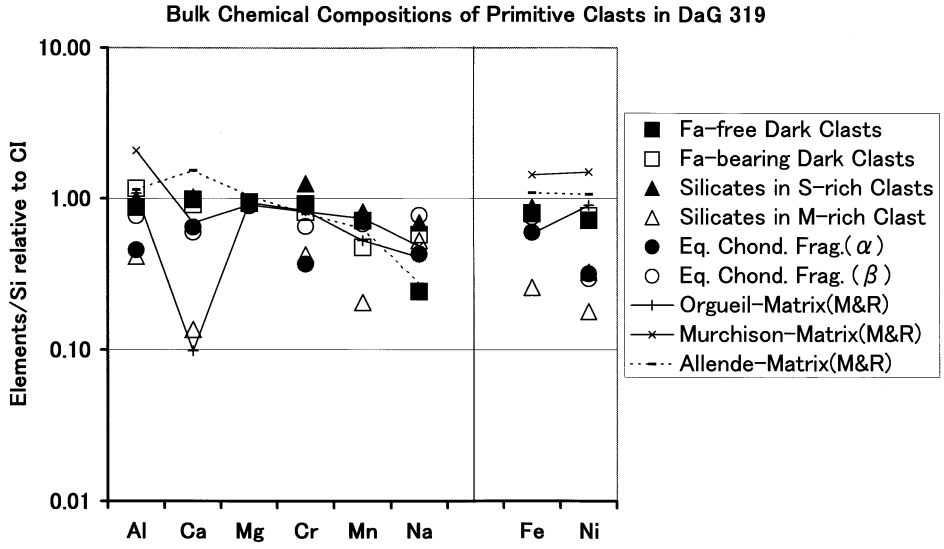

Fig. 6. Bulk chemical compositions of primitive lithic clasts are normalized to Si and CI chondrites with compositions of the Orgueil matrix, the Murchison matrix and the Allende matrix taken from McSween and Richardson (1977; M&R). Abbreviations: silicate-rich matrix (Silicates) in sulfide-rich clasts (S-rich clasts) and metal-rich clasts (M-rich clasts), and two equilibrated chondrite fragments (Eq. Chond. Frag. (α) and (β)).

may be due to enrichment of Si in the silicate-rich matrices of the metal-rich clast.

4.3. Equilibrated chondrite fragments

Major element compositions were determined for two equilibrated chondrite fragments, and their average compositions are similar to each other (Table 3 and Fig. 6). Although some major elements (Al, Cr and Ni) seem to be slightly depleted in comparison with CI chondrite, they may be related to ordinary or R chondrites (Fig. 6).

5. Oxygen isotopic compositions

The oxygen isotopic compositions of primitive clasts in DaG 319 have been obtained by SIMS (Table 4) and are plotted in Fig. 7. Most ureilites plot on an extension of the CCAM mixing line of the Allende meteorite (Clayton and Mayeda, 1988). A dark clast in Nilpena falls at the heavier (^{16}O-poor) oxygen end of the line (Clayton and Mayeda, 1988; Brearley and Prinz, 1992).

The type I and type II ureilitic clasts (usual and unusual monomict ureilitic clasts, respectively; Ikeda *et al.*, 2000) in DaG 319 have oxygen isotopic compositions identical to the monomict ureilites (Kita *et al.*, 2000).

5.1. Sulfide-rich and metal-rich clasts

Oxygen isotopic compositions of olivine from two sulfide-rich clasts (α32A and β26A) were measured. One is a homogeneous grain in β26A and is Fo_{76-77}, the other is zoned olivine in α32A and ranges Fo_{67-79}. The $\delta^{17}O$ of β26A is lower than that of α32A. Olivine in two sulfide-rich clasts and enstatite in one metal-rich clast plot on the CCAM mixing line between the Allende matrix and the Nilpena dark clast (Fig. 7),

Table 4. Oxygen isotopic composition of primitive clasts in the DaG-319 polymict ureilite.

Sample	Clast Type	Mineral	$\delta^{18}O$ ‰		$\delta^{17}O$ ‰		$\Delta^{17}O$ ‰
Sulfide- and metal-rich clasts							
α 32A	Sulfide-rich	Fo79-67	8.96	± 0.82	5.41	± 0.60	0.75
β 26A	Sulfide-rich	Fo76-77	7.42	± 0.25	3.32	± 0.94	-0.54
α 42A	Metal-rich	En98-99	5.85	± 0.84	1.32	± 0.76	-1.72
Unusual chondritic clast							
α 14A	BO chondrule	Fo71-73	2.74	± 0.36	2.67	± 0.80	1.24
α 33B	POP chondrule	Fo82	4.24	± 0.38	2.87	± 1.21	0.66
		Fo82	3.44	± 0.47	2.74	± 0.97	0.96
		average	3.84	± 1.14	2.84	± 0.76	0.84
α 41A	PO chondrule	Fo97-77	4.40	± 0.53	2.71	± 1.87	0.42
		Fo80-73	4.93	± 0.26	3.90	± 1.13	1.34
		average	4.66	± 0.74	3.52	± 0.97	1.09
α 43A	Eq. chondrite	Fo69	3.44	± 0.33	2.47	± 1.41	0.68
β 22B	Eq. chondrite	Fo60	3.55	± 0.37	2.96	± 1.03	1.11

$\Delta^{17}O = \delta^{17}O - 0.52\,\delta^{18}O$, barred olivine (BO), porphyritic olivine and pyroxene (POP), porphyritic olivine (PO), and equilibrated (Eq).

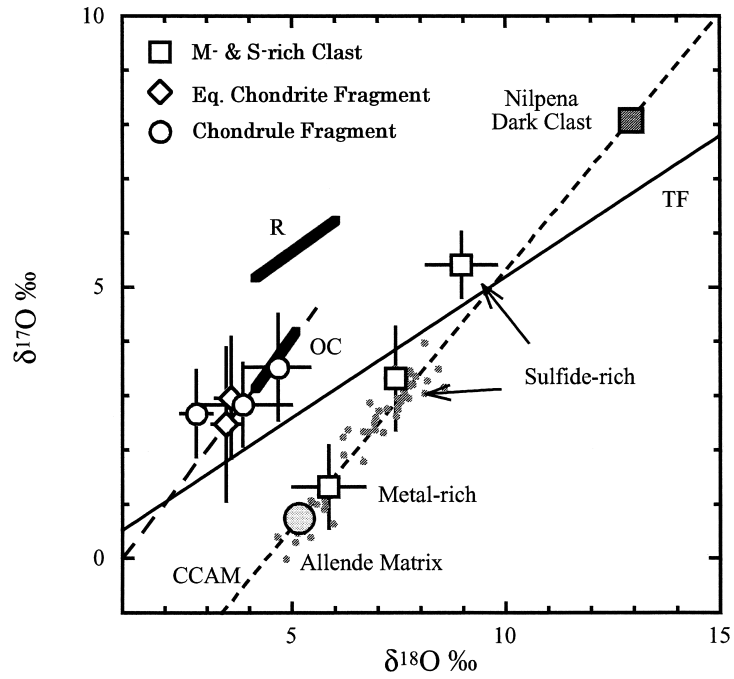

Fig. 7. Three-isotope plot for oxygen in the silicate-rich matrices in the metal-rich and sulfide-rich clasts (M- & S-rich Clast) and unusual chondritic fragments (Chondrule Fragment and Equilibrated Chondrite Fragment), as well as the Nilpena dark clast and the Allende matrix. Compositional ranges of ordinary chondrites (OC), R chondrites (R), and the terrestrial fractionation line (TF) are shown for reference. Usual monomict ureilites (small dots; Clayton and Mayeda, 1988) are plotted along the extension (dashed line) of the Allende mixing line with CCAM (carbonaceous chondrite anhydrous minerals).

suggesting a genetic relationship with the usual monomict ureilites. Enstatite in the metal-rich clast plots near the Allende matrix with the lowest $\delta^{17}O$ (Fig. 7).

5.2. Chondrule and equilibrated chondrite fragments

The chondrule and equilibrated chondrite fragments in DaG 319 have oxygen isotopic compositions very similar to those of ordinary chondrites. It is difficult to distinguish them from H, L, or LL compositions because of relatively large error in the data. They plot at the lower end of the ordinary chondrite trend (Fig. 7), indicating that they might be a sample of ordinary chondritic material, but not exactly the same as ordinary chondrites. However, the average olivine compositions of the chondrite fragments in DaG 319 suggest that they might be related to a more ferroan chondrite group.

6. Discussion

6.1. Precursors of ureilites

The Fa-bearing dark clasts suffered weak hydration, and their matrix contains

ferroan phyllosilicates. The groundmass of the exotic rock fragment in the Fa-bearing dark clast also contains fine-grained ferroan hydrated phyllosilicates with minor amounts of fayalite, suggesting that the groundmass may have suffered hydration at the same time as the host matrix of the Fa-bearing dark clast. The Fa-bearing dark clast probably represent surficial materials from the ureilite parent body (UPB).

The Fa-free dark clasts experienced intense hydration. The common occurrence of phyllosilicate veins in the clasts indicates that the hydration took place in an asteroidal body and not in the nebula. However, it is not clear whether the asteroidal setting is the UPB that produced the DaG 319 polymict breccia or not. The Fa-free dark clasts in DaG 319 are texturally similar to the Nilpena clast, and they may have similar bulk oxygen isotopic compositions. Since the dark clast in Nilpena plots on the heavier (^{16}O-poor) extension of the CCAM mixing line, the dark clasts in both Nilpena and DaG 319 might have a genetic relationship to the UPB. Young and Russell (1998) discussed the mass fractionation trajectory of altered melilites, and their oxygen isotopic compositions are coincident with the CCAM mixing line: the anhydrous melilites were originally on a slope-1 mixing line which is different from the CCAM line, and they deviated toward the CCAM mixing line during the hydration. If the dark clasts in DaG 319 experienced similar hydration temperatures, their anhydrous precursors may have been on a slope-1 mixing line which differs from the CCAM. This would suggest that the anhydrous precursors of the dark clasts might not have a direct genetic relationship to the precursors of the usual monomict ureilites. However, further study of dark clasts in polymict ureilites is needed to decipher their genesis.

The sulfide-rich clasts consist of anhydrous silicate-rich matrix with disseminated sulfide. The matrix has an oxygen isotopic compositions that plots along the CCAM mixing line, near the region of most ureilitic clasts in DaG 319 (Kita *et al.*, 2000), suggesting that the silicate-rich matrix may represent the precursors of the ureilitic clasts at a moderate depth in the UPB. If so, these clasts escaped the partial melting which produced the monomict ureilites, and later suffered sulfurization elsewhere in the UPB.

The metal-rich clasts consist mainly of reduced anhydrous silicates with disseminated metal and sulfide. The silicates have oxygen isotopic compositions that plot along the CCAM mixing line, near Allende matrix, suggesting that the silicates may represent precursors of monomict ureilites having lighter oxygen compositions at a deeper region in the UPB. They also escaped partial melting, and later suffered metal-sulfide dissemination, possibly due to impact-induced shock events on the UPB.

The bulk composition of the silicate-rich matrix in the metal-rich clasts is enriched in SiO_2, as already discussed. This SiO_2-enrichment can be explained by addition of Si from Si-bearing metallic phases which were disseminated into the metal-rich clasts. The addition of Si may take place by the following reaction:

$$\underset{\text{in Metal}}{\text{Si}} + \underset{\text{in Matrix}}{2\text{FeO}} = \underset{\text{in Matrix}}{\text{SiO}_2} + \underset{\text{in Metal}}{2\text{Fe}}. \quad (1)$$

Some of the Si in the metallic phases was used for reduction of FeO in the matrix by eq. (1) to produce enstatite or the silica mineral that commonly occurs in the metal-rich clasts. The rest of Si remained in the metallic phases, explaining that the kamacite in the metal-rich clasts still contains a few wt% of Si.

6.2. Reduction and partial melting residues

Ikeda and Prinz (2001) discussed the origin of ureilites and concluded that the monomict ureilites were produced as residues by fractional partial melting of chondritic precursors. The total partial melting degree may not exceed 30% (Kita *et al.*, 2001). The following discussion assumes that the monomict ureilites are residues of the fractional partial melting.

The precursors of ureilites are considered to have a genetic relationship with a kind of carbonaceous chondrite (Tomeoka and Takeda, 1990). The chondritic precursor may be similar to the sulfide-rich and metal-rich clasts in DaG319 or their silicate-rich matrices, as well as Allende matrix-like materials. Since the matrix of the metal-rich clasts may have suffered Si-addition from metallic phases, the silicate-rich matrix of the sulfide-rich clasts is a better candidate for the ureilite precursors. However, it has an mg ratio of 0.56 and is too ferroan to produce the monomict ureilites. It would have had to experience reduction prior to partial melting to produce ureilites as residues. Carbonaceous materials (hydrocarbons) in the precursors may have acted as reducing agents. The reduction may have taken place at moderate depth in the UPB, with increasing temperatures, due to short-live radioisotopes, as well as heating due to impact bombardment (Scott *et al.*, 1992,1993). The reduction reaction may be expressed by the simplified equation:

$$CH_4 + 3FeO = 3Fe + CO + 2H_2O. \quad (2)$$

For simplicity, we consider the case that half (16.05 wt%) of original FeO (32.10 wt%, Table 3) in the silicate-rich matrix in the sulfide-rich clasts is reduced by eq. (2). The reduced, silicate-rich matrix has an mg ratio of 0.71 (Table 5). This reduction is at least necessary for precursors of usual monomict ureilites, because the lowest mg ratio of usual monomict ureilites is 0.74 (Goodrich, 1992). Fractional partial melting of more highly reduced precursors may result in formation of olivine-pigeonite residues with mg ratios larger than 0.74. The MnO contents of the reduced and original matrices are plotted against their FeO contents in Fig. 8, connected by a dashed line with an arrow. This reduction trend is consistent with the fact that most monomict ureilites fall on a reduction trend shown by a solid line in Fig. 8.

The reduction of FeO (16.05 wt%) of the matrix in the sulfide-rich clasts by eq. (2) may have consumed ~1 wt% hydrocarbons (for simplicity, CH_4). As ureilites contain 0.2 to 6 wt% of carbon (Grady *et al.*, 1983), the original matrix of the sulfide-rich clasts must have contained more than a few wt% carbonaceous materials. The 1–2 wt% was used for the reduction to produce reduced precursors with variable mg ratios, and the rest of the carbonaceous materials may have been used to form the graphitic materials in the ureilite residues (Berkley and Jones, 1982). Reduction by eq. (2) may have taken place pervasively at depth in the UPB, but reduction by eq. (1) may have been localized to where the Si-bearing metallic phases were disseminated.

6.3. Projectiles

Unusual chondritic fragments (chondrule and equilibrated chondrite fragments) have oxygen isotopic compositions that differ from the CCAM mixing line, indicating that they have no direct genetic relationship to the usual monomict ureilites. They

Table 5. Chemical composition (wt%) of a reduced precursor of ureilites estimated from silicate-rich matrix of sulfide-rich clasts. Right column is recalculated to 100 wt% oxides.

	Reduced precursor	
SiO_2	35.14	43.53
TiO_2	0.13	0.16
Al_2O_3	2.50	3.10
Cr_2O_3	0.75	0.93
FeO	16.05	19.88
MnO	0.32	0.40
MgO	22.56	27.95
CaO	1.98	2.45
Na_2O	0.70	0.87
K_2O	0.08	0.10
P_2O_5	0.51	0.63
(Subtotal)	(80.72)	(100.00)
Fe	12.48	metal
Ni	0.55	&
S	0.46	sulfide
Total	94.21	
mg	0.71	

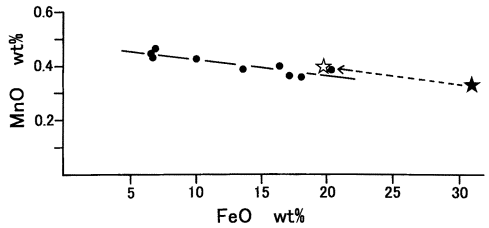

Fig. 8. MnO contents of the silicate-rich matrix in the sulfide-rich clasts (solid star) and a reduced precursor (see text, open star) with a dashed arrow are plotted against their FeO contents. The normalized FeO content (Table 5; 19.88 wt%) of the reduced precursor is used here. Usual monomict ureilites (solid circles) with a regression line are shown for reference. Ureilite data sources: Boynton et al. (1976), Takeda (1987, 1989), and Jarosewich (1990).

were derived from outside of the UPB, and were exotic projectiles that collided with the surface of the UPB to produce clastic matrix breccias or regolith breccias, such as polymict ureilites. The chondrule fragments have the oxygen isotopic compositions similar to the equilibrated chondrite fragments, indicating that both subtypes have a genetic relationship to each other. As already shown, they may be a new type of chondrite that is different from the known chondrite groups.

7. Conclusions

(1) Fa-free dark clasts consist mainly of phyllosilicates, sulfide, magnetite, and carbonates, and they experienced intense hydration in an asteroidal body. Fa-bearing dark clasts contain exotic rock fragments, and the matrix of the Fa-bearing clasts and the groundmass of the exotic fragment suffered weak hydration to produce smectite-rich ferroan phyllosilicates.

(2) The silicate-rich matrices of the sulfide-rich and metal-rich clasts, as well as the Allende matrix-like materials, which are chondrule free and anhydrous, are good candidates to be the precursors of monomict ureilites. They fall on the CCAM mixing line, and may represent different strata ranging from a deep region to the surface of the UPB. Fine-grained materials similar to the Allende matrix can be from the deepest regions, the silicate-rich matrices of the metal-rich and sulfide-rich clasts can be from an intermediate depth, and the dark clasts can be from the surface. The silicate-rich matrix of the sulfide-rich clasts is the best candidate for the parental precursors of the usual monomict ureilites.

(3) Unusual chondritic fragments (chondrules and equilibrated chondrites) have no direct genetic relationship with the ureilites, and may be a new type of chondrite. They were projectiles that collided with the UPB to produce the polymict ureilites such as DaG 319.

Acknowledgments

This study was carried out with the help of grant (No. 10440149) of The Monbu-Kagaku Shou (Ministry of Education, Science, and Culture) to Y. Ikeda, and NASA grant, NAG5-11546, to M.K. Weisberg (PI).

References

Bence, A.E. and Albee, A.L. (1968): Empirical correction factors for the electron microanalysis of silicates and oxides. J. Geol., **76**, 382–403.

Berkley, J.L., Taylor, G.L., Keil, K., Harlow, G.E. and Prinz, M. (1980): The nature and origin of ureilites. Geochim. Cosmochim. Acta, **44**, 1579–1597.

Berkley, J.L. and Jones, J.H. (1982): Primary igneous carbon in ureilites: Petrological implications. Proc. Lunar Planet. Sci. Conf., 13th, Pt. I, A353–A364 (J. Geophys. Res., **87**, Suppl.).

Bischoff, A., Geiger, T., Palme, H., Spettel, B., Schulz, L., Scherer, P., Loeken, T., Bland, P., Clayton, R.N., Mayeda, T.K., Herpers, U., Meltzow, B., Michel, R. and Dittrich-Hannen, B. (1994): Acfer 217-A new member of the Rumuruti chondrite group (R). Meteoritics, **29**, 264–274.

Boynton, W.V., Starzyk, P.M. and Schmitt, R.A. (1976): Chemical evidence for the genesis of the ureilites, the achondrite Chassigny and the nakhlites. Geochim. Cosmochim. Acta, **40**, 1439–1447.

Brearley, A.J. and Prinz, M. (1992): CI chondrite-like clasts in the Nilpena polymict ureilites for aqueous alteration process in CI chondrites. Geochim. Cosmochim. Acta, **56**, 1373–1386.

Brearley, A.J. and Jones, R.H. (1998): Chondritic meteorites. Rev. Mineral., **36**, 3.1–3.398.

Choi, B-G., Krot, A.N. and Wasson, J.T.(2000): Oxygen isotopes in magnetite and fayalite in CV chondrites Kaba and Mokoia. Meteorit. Planet. Sci., **35**, 1239–1248.

Clayton, R.N., Onuma, N., Ikeda, Y., Mayeda, T.K., Hutcheon, I.D., Olsen, E.J. and Molini-Velsco, C.A.

(1983): Oxygen isotopic compositions of chondrules in Allende and ordinary chondrites. Chondrules and Their Origin, ed. by E.A. King. Houston, Lunar Planet. Inst., 37–43.
Clayton, R.N. and Mayeda, T.K. (1988): Formation of ureilites by nebular processes. Geochim. Cosmochim. Acta, **52**, 1313–1318.
Cole, K.J. and Sipiera, R.P. (2002): Classification of ten recent meteorite finds from Dar al Gani, Libya. Meteorit. Planet. Sci., **37**, A37 (abstract).
Goodrich, C.A., Jones, J.H. and Berkley, J.L. (1987): Origin and evolution of the ureilite parent magmas: Multi-stage igneous activity on a large parent body. Geochim. Cosmochim. Acta, **51**, 2255–2273.
Goodrich, C.A. (1992): Ureilites: A critical review. Meteoritics, **27**, 327–352.
Goodrich, C.A., Krot, A.U., Scott, E.R.D., Taylor, G.J., Fioretti, A.M. and Keil, K. (2002): Formation and evolution of the ureilite parent body and its offspring. Lunar and Planetary Science XXIII. Houston, Lunar Planet.Inst., Abstract, #1379 (CD-ROM).
Grady, M.M., Wright, I.P., Swart, P.K. and Pillinger, C.T. (1985): The carbon and nitrogen isotopic composition of ureilites: implications for their genesis. Geochim. Cosmochim. Acta, **49**, 903–915.
Hua, X. and Buseck, P.R. (1995): Fayalite in the Kaba and Mokoia carbonaceous chondrites. Geochim. Cosmochim. Acta, **59**, 563–578.
Ikeda, Y. (1980): Petrology of Allan Hills-764 chondrite (LL3). Mem. Natl Inst. Polar Res., Spec. Issue, **17**, 50–82.
Ikeda, Y., Prinz, M. and Nehru, C.E. (2000): Lithic and mineral clasts in the Dar Al Gani (DAG) 319 polymict ureilite. Antarct. Meteorite Res., **13**, 177–221.
Ikeda, Y. and Prinz, M. (2001): Magmatic inclusions and felsic clasts in the Dar al Gani polymict ureilite. Meteorit. Planet. Sci., **36**, 1–20.
Jaques, A. and Fitzgerald, M.J. (1982): The Nilpena ureilite, and unusual polymict breccia: Implications for origin. Geochim. Cosmochim. Acta, **46**, 893–900.
Jarosewich, E. (1990): Chemical analyses of meteorites: A compilation of stony and iron meteorite analyses. Meteoritics, **25**, 323–338.
Kita, N.T., Liu, Y.Z., Ikeda, Y., Prinz, M. and Morishita, Y. (2000): Identification of variety of clasts in a polymict ureilite using the secondary ion mass spectrometer oxygen isotopic analyses. Meteorit. Planet. Sci., **35**, Suppl., A88–A89.
Kita, N.T., Togashi, Y., Ikeda, Y. and Morishita, Y. (2001): Trace element abundance in plagioclase from the DaG 319 polymict ureilite. In 11th Annual V. M. Goldschmidt Conference, LPI Contribution No. 1088, Abstract #3577, Houston, Lunar Planet. Inst.
Krot, A.N., Petaev, M.I., Zolensky, M.E., Keil, K., Scott, E.R.D. and Nakamura, K. (1998): Secondary calcium-iron-rich minerals in the Bali-like and Allende-like oxidized CV3 chondrites and Allende dark inclusions. Meteorit. Planet. Sci., **33**, 623–645.
Krot, A.N., Brearly, A.J., Petaev, M.I., Kallemeyn, G.W., Sears, D.W.G., Benoit, P.H., Hutcheon, I.D., Zolensky, M.E. and Keil, K. (2000): Evidence for low-temperature growth of fayalite and hedenbergite in MacAlpine Hills 88107, an ungrouped carbonaceous chondrites related to CM-CO clan. Meteorit. Planet. Sci., **35**, 1365–1386.
Kurat, G. (1988): Primitive meteorites: An attempt towards unification. Philos. Trans. R. Soc. London, Ser. A, A325–482.
McSween, H.Y. and Richardson, S.M. (1977): The composition of carbonaceous chondrite matrix. Geochim. Cosmochim. Acta, **41**, 1145–1161.
Mittlefehldt, D.W. (1986): Fe-Ng-Mn relations of ureilite olivine and pyroxenes and the genesis of ureilites. Geochim. Cosmochim. Acta, **50**, 107–110.
Prinz, M., Delaney, J.S., Nehru, C.E. and Weisberg, M.K. (1983): Enclave in the Nilpena polymict ureilite. Meteoritics, **18**, 376–377.
Prinz, M., Weisberg, M.K., Nehru, C.E. and Delaney, J.S. (1986): North Haig and Nilpena: Paired polymict ureilites with Angra Dos Reis-related and other clasts. Lunar and Planetary Science XVII. Houston, Lunar Planet. Inst., 681–682.
Prinz, M., Weisberg, M.K., Nehru, C.E. and Delaney, J.S. (1987): EET 83309, a polymict ureilite: recognition of a new group. Lunar and Planetary Science XVIII. Houston, Lunar Planet. Inst., 802–803.
Rubin, A.E. (1988): Formation of ureilites by impact-melting of carbonaceous chondritic materials.

Meteoritics, **23**, 333–338.
Rubin, A.E. and Kallemeyn, G.W. (1989): Carlisle Lakes and Alan Hills 85151: Members of a new chondrite grouplet. Geochim. Cosmochim. Acta, **53**, 3035–3044.
Scott, E.R.D., Keil, K. and Taylor, G.J. (1992): Origin of ureilites by partial melting and explosive volcanism on carbon-rich asteroids. Lunar and Planetary Science XXIII. Houston, lunar Planet. Inst., 1253–1254.
Scott, E.R.D., Taylor, G.J. and Keil, K. (1993): Origin of ureilite meteorites and implications for planetary accretion. Geophys. Res. Lett., **20**, 415–418.
Singletary, S.J. and Grove, T.L. (2002): Experimental constraints on the genesis of the olivine-pigeonite bearing ureilites. Lunar and Planetary Science XXXIII. Houston, Lunar Planet. Inst., Abstract, #1382 (CD-ROM).
Stöffler, D., Knöll, H.D. and Maerz, U. (1979): Terrestrial and lunar impact breccia and the classification of lunar highland rocks. Proc. Lunar Planet. Sci. Conf., 10th, 639–675.
Takeda, H. (1987): Mineralogy of Antarctic ureilites and a working hypothesis for their origin and evolution. Earth Planet. Sci. Lett., **81**, 358–370.
Takeda, H. (1989): Mineralogy of coexisting pyroxenes in magnesian ureilites and their formation conditions. Earth Planet. Sci. Lett., **93**, 181–194.
Tomeoka, K. and Takeda, H. (1990): Fe-S-Ca-Al-bearing carbonaceous vein in the Yamato-74310 ureilite: Evidence for a genetic link to carbonaceous chondrites. Geochim. Cosmochim. Acta, **54**, 1475–1481.
Van Schmus, W.R. and Ribbe, P.H. (1968): The composition and structural state of feldspar from chondritic meteorites. Geochim. Cosmochim. Acta, **32**, 1327–1342.
Walker, D. and Grove, T. (1993): Ureilite smelting. Meteoritics, **28**, 629–636.
Warren, P.H. and Kallemeyn, G.W. (1989): Geochemistry of polymict ureilite EET83309, and a partially-disruptive impact model for ureilite origin. Meteoritics, **24**, 233–246.
Wasson, J.T., Chou, C.L., Bild, R.W. and Baedicker, P.A. (1976): Classification of and elemental fractionation among ureilites. Geochim. Cosmochim. Acta, **40**, 1449–1458.
Weisberg, M.K. and Prinz, M. (1998): Fayalitic olivine in CV chondrite matrix and dark inclusions: A nebular origin. Meteorit. Planet. Sci., **33**, 1087–1099.
Weisberg, M.K., Prinz, M., Kojima, H., Yanai, K., Clayton, R.N. and Mayeda, T.K. (1991): The Carlisle Lakes-type chondrites: A new grouplet with high $\Delta^{17}O$ and evidence for nebular oxidation. Geochim. Cosmochim. Acta, **55**, 2657–2669.
Young, E.D. and Russell, S.S. (1998): Oxygen reservoirs in the early solar nebula inferred from an Allende CAI. Science, **282**, 452–455.

(Received November 22, 2002; Revised manuscript accepted February 3, 2003)